Available online at www.sciencedirect.com
SCIENCE DIRECT®
Inorganica Chimica Acta 352 (2003) 129–135
Inorganica Chimica Acta
www.elsevier.com/locate/ica

Switchable cycloplatinated ferrocenylamine derivatives of acridone, naphthalimide and anthraquinone

Elise M. McGale, R. Eva Murray, C. John McAdam, Joy L. Morgan, Brian H. Robinson *, Jim Simpson

Department of Chemistry, University of Otago, PO Box 56, Dunedin, New Zealand

Received 6 August 2002; accepted 30 September 2002

Dedicated in honor of Professor Martin A. Bennett

Abstract

Acridone, naphthalimide and anthraquinone derivatives of the cycloplatinated ferrocenylamine {Pt[(η^5-CpFe(σ,η^5-$C_5H_3CH_2NMe_2$)](dmso)C≡C–} have been prepared and the X-ray structure for the anthraquinone derivative has been determined. Spectroelectrochemistry has been used to probe the ground and excited states of these molecules. Irrespective of whether the fluorophore is bound to the ethynylPt(II) link via a nodal nitrogen (acridone) or to the aromatic ring (naphthalimide and anthraquinone) fluorophore emission is quenched in the ground state and partially restored in the oxidised species. Low energy donor-acceptor charge-transfer bands of the oxidised compounds are characteristic.

Keywords: Cycloplatination; Ferrocenylamine; Spectroelectrochemistry; Acridone; Naphthalimide; Anthraquinone

1. Introduction

Cycloplatinated ferrocenylamines **1** offer a redox center which undergoes a reversible one-electron oxidation to a stable cation [1]. The HOMO is essentially centered on the ferrocenyl moiety and lowered in energy relative to a non-cycloplatinated ferrocenylamine by the donor Pt(II) substituent. Furthermore, there are rigid ligand preferences in the *trans* Pt–N and *trans* Pt–L positions for π-acceptors and σ-donors, respectively [1–3]. As a consequence, this redox centre can be tuned by a judicious choice of ligands coordinated to the platinum(II) giving a potential range of 0.01 to ~0.50 volts against decamethylferrocene. The archetypal redox centre $[Fc]^{+/0}$ has been found to induce molecular switching in ferrocenyl–ethynyl–fluorophore dyads [4–6]. We were, therefore, interested to see if emissive assemblages where **1** was the redox center would also function in a similar fashion. Targeted fluorophores for the dyads were acridone, where **1** could be attached at the nitrogen atom, *N*-methylnaphthalimide and anthraquinone, where **1** could be attached to the π-system.

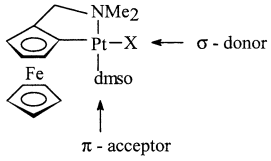

X = Cl **1a**, C≡CH **1b**, C≡CPh **1c**

2. Experimental

The compounds 10-(2-propynyl)-9-acridone [7], 2-iodoacridone [8], 4-trimethylsilylethynyl-*N*-methyl-1,8-naphthalimide [9], **1a** [1] and **1c** [3] were prepared by literature procedures. 4-Ethynyl-*N*-methyl-1,8-naphthalimide was prepared in an analogous way to the 4-ethynyl-1,8-naphthalimides reported previously [10].

* Corresponding author. Tel.: +63-3-4797 907; fax: +63-3-4797 906.
E-mail address: brobinson@alkali.otago.ac.nz (B.H. Robinson).

0020-1693/03/$ - see front matter
doi:10.1016/S0020-1693(03)00152-X

Microanalyses were carried out by the Campbell Microanalytical Laboratory, University of Otago. ^{1}H and ^{195}Pt NMR spectra were recorded on Varian Unity Inova 300 and 500 MHz spectrometers, respectively, in $CDCl_3$ at 25 °C; $\delta^{195}Pt$ data are referenced to K_2PtCl_6. IR and UV–Vis spectra were recorded on a Perkin-Elmer spectrum BX FT-IR and a Varian Cary 500 scanning spectrophotometer, respectively. Electron impact mass spectra were recorded on a Kratos MS80RFA and electrospray mass spectra on a Shimadzu LCMS-QP 8000 spectrometer. Cyclic and square wave voltammetry in CH_2Cl_2 were performed using a three-electrode cell with a polished disk, Pt (2.27mm^2) as the working electrode; solutions were $\sim 10^{-3}$ M in electroactive material and 0.10 M in supporting electrolyte (triply recrystallised $TBAPF_6$). Data was recorded on a Powerlab/4sp computer-controlled potentiostat. Scan rates of 0.05–1 V s^{-1} were typically employed for cyclic voltammetry and for Osteryoung square-wave voltammetry, square-wave step heights of 1–5 mV, a square amplitude of 15–25 mV with a frequency of 30–240 Hz. All potentials are referenced to decamethylferrocene; $E_{1/2}$ for sublimed ferrocene was 0.55 V. Infrared and UV–Vis OTTLE data were obtained from standard cells with platinum grid electrodes. Fluorescence measurements were conducted on optically dilute samples (absorbance < 0.05) in spectroscopic grade solvents on a Perkin-Elmer luminescence spectrometer LS50B. The quantum yield was calculated by comparing the integrated fluorescence spectra with a comparable compound, 4-piperidino-*N*-methyl-1,8-naphthalimide ($\phi_f = 0.91$).

2.1. Preparation of {Pt[(η^5-CpFe(σ,η^5-$C_5H_3CH_2NMe_2$)](dmso)[10-(2-propynyl)-9(10H)-acridinone]}

Compound **1a** (0.120 g, 0.2 mmol) and 10-(2-propynyl)-9(10H)-acridone (0.047 g, 0.2 mmol) were stirred for 3 h at room temperature (r.t.) with CuI (0.0038 g, 0.02 mmol) in degassed piperidine (10 ml). The solvent was removed in vacuo and the residue taken up in CH_2Cl_2 the organic layer washed with water, dried over $MgSO_4$ and the solvent removed in vacuo. The residue separated using column chromatography on alumina; the first band eluted with ethylacetate gave **2** which was recrystallised in CH_2Cl_2 layered with EtOH (0.084 g, 28%). *Anal.* Calc. for $C_{31}H_{32}N_2O_2SFePt$: C, 49.70; H, 4.31; N, 3.75. Found: C, 49.53; H, 4.74; N, 3.69%. ^{1}H NMR ($CDCl_3$, ppm): 2.82, 3.16 {2 × [s, 3*H*, $^{3}J_{Pt-H} = 18$ Hz, N–C*H*$_3$]}, 3.37, 3.44 {2 × [s, 3*H*, Pt satellites $J = 12$ Hz, S–C*H*$_3$]}, 3.73 (d, 2*H*, $J = 14$ Hz, –C*H*$_2$), 4.06 (s, 5*H*, η^5-C$_5$*H*$_5$Fe), 4.10 (d, 2*H*, $J = 2$ Hz, η^5-C$_5$*H*$_3$Fe), 4.30 (t, 1*H*, $J = 2$ Hz, η^5-C$_5$*H*$_3$Fe), 5.08 (s, 2*H*, –C*H*$_2$–N), 7.32 (m, 2*H*, acridone-*H*), 7.76 (dd, 4*H*, $J = 5.4$, 1 Hz, acridone–*H*), 8.57 (dt, 2*H*, $J = 8$, 1 Hz, acridone–*H*). ^{195}Pt NMR ($CDCl_3$, ppm): −3755. IR (CH_2Cl_2, cm^{-1}): $\nu_{(C=O,\ C=N)}$ 1632, 1601. $\nu_{(C\equiv C)}$ 2114. UV–Vis (CH_2Cl_2, λ_{max}, nm, ε 1 $mol^{-1}cm^{-1}$): 399 (923), 255 (4173). $E^{+/0}$ (CH_2Cl_2, V): 0.27.

Table 1
Crystallographic data for **5**

Empirical formula	$C_{31}H_{29}NO_3SFePt$
Formula weight	746.55
Crystal system	triclinic
Space group	$P\bar{1}$
Unit cell dimensions	
a (Å)	10.050(2)
b (Å)	12.616(3)
c (Å)	20.999(4)
α (°)	94.04(3)
β (°)	99.87(3)
γ (°)	93.04(3)
V (Å^3)	2610.8(9)
Z	4
D_{calc} (Mg m^{-3})	1.899
μ(Mo Kα) (mm^{-1})	6.023
$F(000)$	1464
Temperature (K)	168(2)
Crystal size (mm^3)	0.34 × 0.20 × 0.04
θ Range (°)	1.97–26.54
Total reflections	11613
Independent reflections	9232
R_{int}	0.0750
No. parameters	343
GoF (F^2)	1.043
R_1 [$I > 2\sigma(I)$]	$R_1 = 0.1071$
wR_2 (all data)	$wR_2 = 0.3398$
Residuals (e Å^{-3})	8.004 and −4.556

2.2. Preparation of {Pt[(η^5-CpFe(σ,η^5-$C_5H_3CH_2NMe_2$)](PPh$_3$)[10-(2-propynyl)-9(10H)-acridinone]}

Triphenylphosphine (0.013 g, 0.05 mmol) was added to **2** (50 mg, 0.05 mmol) in CH_2Cl_2 (20 ml) and the solution was stirred for 3 h at r.t. The solvent was removed in vacuo and **3** recrystallised in CH_2Cl_2 layered with EtOH. (39 mg, 83%). *Anal.* Calc. for $C_{47}H_{41}N_2OPFePt$: C, 60.58; H, 4.44; N, 3.00. Found: C, 60.30; H, 4.55; N, 2.81%. ^{1}H NMR ($CDCl_3$, ppm): 2.88, 2.95 {2 × [s, 1*H*, –C*H*–]}, 3.11, 3.35 {2 × [d, 3*H*, $J = 3$ Hz, $^{3}J_{Pt-H} = 12$ Hz, N–C*H*$_3$]}, 3.78 (s, 5*H*, η^5-C$_5$*H*$_5$Fe), 3.78 (m, 3*H*, η^5-C$_5$*H*$_3$Fe), 4.02 (m, 3*H*, η^5-C$_5$*H*$_3$Fe), 4.66 (d, 2*H*, $J = 2$ Hz, –C*H*$_2$), 7.21–7.40 (m, 13*H*, Ph–*H*), 7.52–7.59 (m, 2*H*, acridone–*H*), 7.63–7.70 (m, 6*H*, 4 × acridone–*H*, 2 × Ph–*H*) 8.50 (dd, 2*H*, $J = 8$, 2 Hz, acridone–*H*). ^{195}Pt NMR ($CDCl_3$, ppm): –4232. IR (CH_2Cl_2, cm^{-1}): $\nu_{C=O,\ C=N}$, 1632, 1601; $\nu_{(C\equiv C)}$ 2114. UV–Vis (CH_2Cl_2, λ_{max}, nm, ε l $mol^{-1}cm^{-1}$): 403 (712), 383 (569), 256 (2970). $E^{+/0}$ (CH_2Cl_2, V): 0.23.

2.3. Preparation of {Pt[(η^5-CpFe(σ,η^5-$C_5H_3CH_2$-NMe_2)](dmso)[4-ethynyl-N-methyl-1,8-naphthalimide]}

4-Ethynyl-*N*-methyl-1,8-naphthalimide (0.055 g, 0.23 mmol) and **1a** (0.119 g, 0.22 mmol) were stirred in 20 ml dried, degassed triethylamine with 5% CuI at r.t. for 24 h. The solvent was removed from the deep red–brown reaction mixture under reduced pressure, the resulting solid dissolved in CH_2Cl_2 and washed six times with 20 ml H_2O to remove any remaining triethylamine. The solution was then treated with $MgSO_4$, filtered and the solvent removed in vacuo. Recrystallisation from hot methanol gave **4** as a dark purple–brown crystalline solid (0.11 g, 67%). *Anal.* Calc. for $C_{30}H_{32}PtFeN_2O_3S$: C, 47.94; H, 4.29; N, 3.73; S, 4.27. Found: C, 47.53; H, 4.33; N, 3.77; S, 4.08%. EI MS: *m/z* 749 $[M]^+$. ^{1}H NMR ($CDCl_3$, ppm): 3.08 (s, 3H, $^3J_{Pt-H} = 36$ Hz, NCH_3), 3.46 (s, 3H, NCH_3), 3.55 (s, 3H, naphth–NCH_3), 3.70 (s, 3H, SCH_3), 3.76 (s, 3H, SCH_3), 3.88 (AB, 2H, $J_{AB} = 13.8$ Hz, NCH_2), 4.16 (m, 5H, η^5-C_5H_5Fe), 4.19 (m, 2H, two of η^5-C_5H_3Fe), 4.42 (m, 1H, one of η^5-C_5H_3Fe), 7.74 (m, 2H, naphth.), 8.47 [d (J = 7.8Hz), 1H, naphth.], 8.60 [d ($J = 7.2$ Hz), 1H, naphth.], 8.78 [d ($J = 7.5$ Hz), 1H, naphth.]. ^{195}Pt NMR ($CDCl_3$, ppm): −3717. IR (CH_2Cl_2, cm^{-1}): $\nu_{C\equiv C}$ 2083, $\nu_{C=O}$ 1694, 1656, $\nu_{S=O}$ 1128. UV–Vis (CH_2Cl_2; λ_{max}, nm, ε l mol^{-1}cm^{-1}): 250 (30,300), 284 (17,400), 350 (810), 408 (25,500). $E^{+/0}$ (CH_2Cl_2, V): 0.22.

2.4. Preparation of {Pt[(η^5-CpFe(σ,η^5-$C_5H_3CH_2NMe_2$)](dmso)[2-ethynyl-anthraquinone]}

2-Ethynyl-anthraquinone (0.112 g, 0.48 mmol) and **1a** (0.266 g, 0.48 mmol) were refluxed in dried, degassed piperidine (10 ml) with 5% CuI for 5 h. The solvent was removed under reduced pressure, and the resulting solid was purified using column chromatography on alumina; the first band eluted with ethylacetate gave **5** which was recrystallised in CH_2Cl_2 layered with hexane (0.145 g, 40%). *Anal.* Calc. for $C_{31}H_{29}FeNO_3PtS$: C, 49.87; H, 3.92; N, 1.88; S, 4.29. Found: C, 49.86; H, 3.92; N, 2.01; S, 3.96%. ES MS: *m/z* 746 $[M]^+$ (74%) 745 $[M-H]^+$ (100%). ^{1}H NMR ($CDCl_3$, ppm): 2.89 (s, 3H, $^3J_{Pt-H}$ = 18 Hz, NCH_3), 3.22 (s, 3H, $^3J_{Pt-H} = 18$ Hz, NCH_3), 3.42 (s, 3H, SCH_3), 3.49 (s, 3H, SCH_3), 3.53 (m, 2H, NCH_2), 4.15 (s, 5H, C_5H_5), 4.18 (m, 2H, two of η^5-C_5H_3Fe), 4.43 (m, 1H, one of η^5-C_5H_3Fe), 7.67 (dd, 1H, $J = 8$, 2 Hz, anth.), 7.80 (m, 2H, anth.), 8.19 (dd, 2H, $J = 8$, 2 Hz, anth.), 8.31 (m, 2H, anth.). ^{195}Pt NMR ($CDCl_3$, ppm): −3699. IR (CH_2Cl_2, cm^{-1}): $\nu_{C\equiv C}$ 2094, $\nu_{C=O}$ 1673, $\nu_{S=O}$ 1131. UV–Vis (CH_2Cl_2; λ_{max}, nm, ε l mol^{-1}cm^{-1}): 305 (25,200), 403 (7000). $E^{+/0}$ (CH_2Cl_2, V): 0.30.

2.5. X-ray data collection, reduction and structure solution for 5

Crystal data for **5** are given in Table 1. Recrystallisation from dichloromethane/ethyl acetate layered with hexane, yielded dark brown plates one of which was used for data collection. Data was collected at 168 K on a Bruker SMART CCD diffractometer, processed using XSCANS [11].

Analysis of the reflection data revealed substantial twinning in the crystal. A unique cell was subsequently found and the associated reflections chosen using the program RLAT [12], these were used in the subsequent solution and refinement process. The structure was solved in the non-centric space group $P\bar{1}$ by Patterson methods using SHELXS [13]. Early stages of the refinement indicated that the non-centric alternative $P\bar{1}$ would be more appropriate; conversion $P\bar{1}$ and full-matrix least-squares refinement using SHELXL-97 [14] and TITAN2000 [15] revealed all atoms of the two unique molecules in the triclinic unit cell. Pt, Fe and S atoms were assigned anisotropic temperature factors and the H atoms were included in calculated positions with isotropic temperature factors 1.2 times that of U_{iso} of the atoms to which they are bound. A number of high peaks were found in the final difference map close to the heavy atoms reflecting the lack of absorption corrections on the data.

3. Results and discussion

Synthetic strategies for the preparation of **2**–**5** are shown in Schemes 1–3. The synthesis of the ynamine **2** was achieved via a CuI-catalysed reaction between 10-(2-propynyl)-9-acridone and **1a** (Scheme 2). This route, rather than one between **1b** and acridone, avoids the problem of β-adduct formation which are the principal products with ferrocenyl analogues [6]. Replacement of the dmso ligand in the *trans* Pt–N position by the stronger π-acceptor PPh_3 gave **3**. Only ynamine complexes of acridone were accessible as attempts to prepare a 2-ethynylacridone derivative via coupling reactions of **1b** with 2-iodoacridone were unsuccessful. However, Sonogashira coupling reactions were a convenient, high-

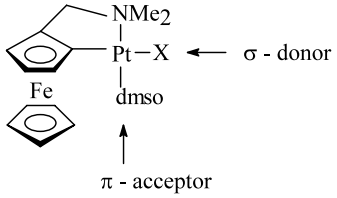

X = Cl **1a**, C≡CH **1b**, C≡CPh **1c**

Scheme 1.

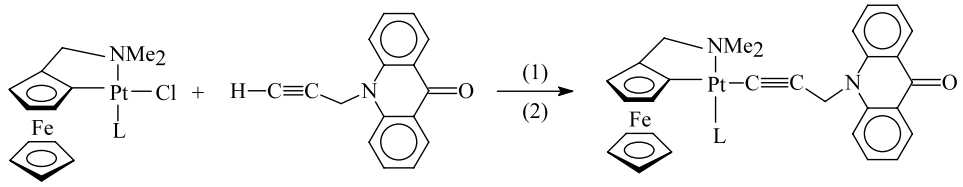

(1) CuI (2) piperidine L = dmso **2**; PPh_3 **3**

Scheme 2.

yield synthetic route to complexes of naphthalimide **4** and anthraquinone **5** (Scheme 3).

All compounds were stable in air and soluble in chlorinated solvents, acetone and alcohols. They were fully characterised by elemental analysis, EI MS, ^{1}H NMR, ^{195}Pt NMR and IR spectroscopy. The $\nu_{PtC\equiv C}$ energies were typical of a σ,η^1-acetylide group although dependent on the Pt–C≡C terminal substituent. For the strong acceptors, naphthalimide and anthraquinone, $\nu_{C\equiv C}$(**4**,**5**) = 2083 cm^{-1} shifting to higher energy $\nu_{C\equiv C}$(**2**) = 2112 cm^{-1} for the weaker acceptor, an *N*-bound acridone. As has been noted elsewhere [3], $\nu_{PtC\equiv C}$ is insensitive to the orthogonal π-acceptor ligand and $\nu_{C\equiv C}$ = 2112 cm^{-1} for both **2** and **3**. The $\nu_{(C=O,\ C=N)}$ bands for the acridone and naphthalimide unit were typical of the parent molecules showing that there was little perturbation of their electronic structure by the cycloplatinated ethynyl group. There was a small upfield shift from δ^{195}Pt(1) at −3763 ppm, because of the stronger electron acceptor and π-donor in the *trans* Pt–C position; δ^{195}Pt(2) −3725, 5 −3717 (cf. −3700 for **1c** [3]). Replacement of dmso in the *trans*-Pt–N position by a π-acceptor causes a large downfield shift to δ^{195}Pt(3) = −4232 as expected.

3.1. Spectroelectrochemistry

Compounds **2**–**5** display chemically reversible one-electron oxidation processes in their cyclic and square wave voltammetry. The potentials (Table 1) are similar to other cycloplatinated ferrocenylamines and the observed oxidation step is assigned to the ['Fc']$^{+/0}$ couple {hereafter 'Fc' = Pt[(η^5-CpFe(σ,η^5-$C_5H_3CH_2NMe_2$)]}. The cathodic shift in the ['Fc']$^{+/0}$ potential from [**1a**]$^{+/0}$ to [**1c**]$^{+/0}$ is due[3] to the acetylide anion being a more effective π-donor than Cl^-. This π-donor ability is apparently ameliorated by the electron-acceptor acetylide substituents acridone or anthraquinone such that [**2**]$^{+/0}$ and [**5**]$^{+/0}$ lie between [**1a**]$^{+/0}$ and [**1c**]$^{+/0}$. As a caveat, the π-donor capability appears to be unaffected by attachment of the electron-acceptor directly to the 'aromatic' ring system or as an ynamine. Nonetheless, [**4**]$^{+/0}$ = [**1c**]$^{+/0}$, that is, cathodic of [**1a**]$^{+/0}$ even though a naphthalimide is a strong electron acceptor. B3LYP calculations [16] indicate that the similarity between **2** and **5** and their weaker π-donor capability relative to **4** is a reflection of the poor π-orbital extension of the acetylide ligand to the Pt(II) coordination centre in **2** and **5**. The acetylide orbital profile for **4** is very similar

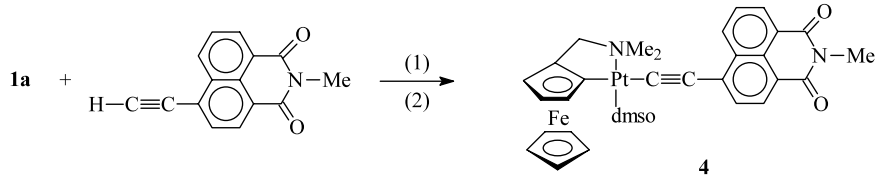

4

(1) CuI (2) Et_3N

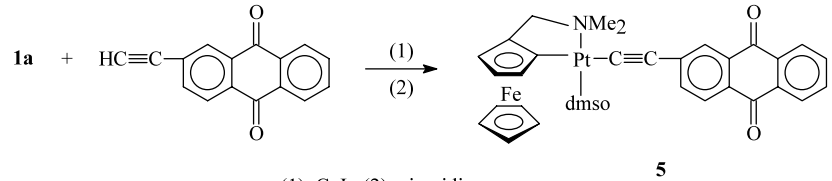

5

(1) CuI (2) piperidine

Scheme 3.

to that in **1c**. Substitution of the *trans* Pt–N ligand, dmso, in **2** by a good π-acceptor decreases the electron density on 'Fc' with an anodic shift to 0.27V from **2** to **3**, in agreement with other cycloplatinated systems [2].

Compounds **2**–**5** also show one-electron irreversible reduction processes > -1.00 V at potentials comparable to the reduction potentials of the parent fluorophores. Radical anions of **2** and **4** were obtained by in situ electroreduction in the ESR cavity and in both cases the ESR parameters were the same as those for the parent fluorophore anions [17] under the same conditions. This clearly demonstrates that the LUMO in the ground state is a fluorophore-based orbital.

Electronic spectra of **2**–**5** are given in Table 2. The energies of the π–π* or n–π* bands in neutral **2**–**5** are relatively unperturbed from the parent ethynylfluorophore. This supports the conclusion from the electrochemistry and IR data that there is little communication between the Pt(II) unit and the fluorophore. In the ground state the HOMO is essentially a 'Fc' orbital. 'Fc' compounds characteristically [1,2] have two transitions at 450–470 and <350 nm and the energy of these is relatively invariant with the ligands around the Pt(II) coordination sphere. With the acridone compounds, these transitions are subsumed by the strong n–π* transitions of the fluorophore; in **4** the 'ferrocenyl' band is only seen as an ill-defined shoulder.

Spectroelectrochemical oxidation of each compound in-situ in OTTLE cells, or by chemical oxidation, caused significant changes in the electronic spectra (Fig. 1). The spectra generated had well-defined isosbestic points and were reversible, indicating that the oxidised species is reasonably stable in this timeframe. Oxidation consistently caused a blue shift of the π–π* and n–π* bands. Because of overlapping bands in the 400–500 nm region it is difficult to comment on changes to the 'Fc' bands

Table 2
$E^{+/0}$ and electronic spectral data

Compound	$E^{+/0}$ (V)	λ_{max} (ε^1) neutral	λ_{max} (ε^1) oxidised	CT band
1a	0.33	449 (*2.4*)		
1c	0.22	465 (3.4)	395 (1320), 480 (540)	
2	0.27	378 (108), 398 (4.3)	396, 475	768
3	0.23	384 (130), 401 (4.9)	401	836
4	0.22	350 (81.4), 408 (255)	411, 592	773
5	0.30	305 (252), 403 (70)	297, 395	768

In CH_2Cl_2 at 20 °C; E° (V) (referenced against decamethylferrocene, Pt, CV data, 200 mV s^{-1}); λ (nm), $\varepsilon \times 10^{-2}$ l mol^{-1} cm^{-1}.

although there appeared to be a small red shift. However, the most important feature of the spectra of $\mathbf{2}^+$–$\mathbf{5}^+$ was the appearance of a broad low energy band in the NIR around 800–900 nm (Table 2, Fig. 1). This band is absent in non-polyaromatic complexes of 'Fc'$^+$ but a similar type of transition has been seen in other oxidised ferrocenylethynyl–dyads with polyaromatics as donors. These low energy bands in the electronic spectra of $\mathbf{2}^+$–$\mathbf{5}^+$ show negative solvatochromism, typical behaviour of charge-transfer transitions in which the excited state is less polar than the ground state [18]. Consequently, these bands in the oxidised species can be assigned to a donor-acceptor transition 'Fc'$^+$ ←(C≡C–R) from the HOMO of the fluorophore to an orbital largely on the 'Fc' moiety.

Fluorescence is totally quenched in the ground state of **2**–**5**. Upon oxidation to $\mathbf{2}^+$–$\mathbf{5}^+$ there was a red-shift of the emission wavelength relative to the parent fluorophore and a slight enhancement of fluorescence.

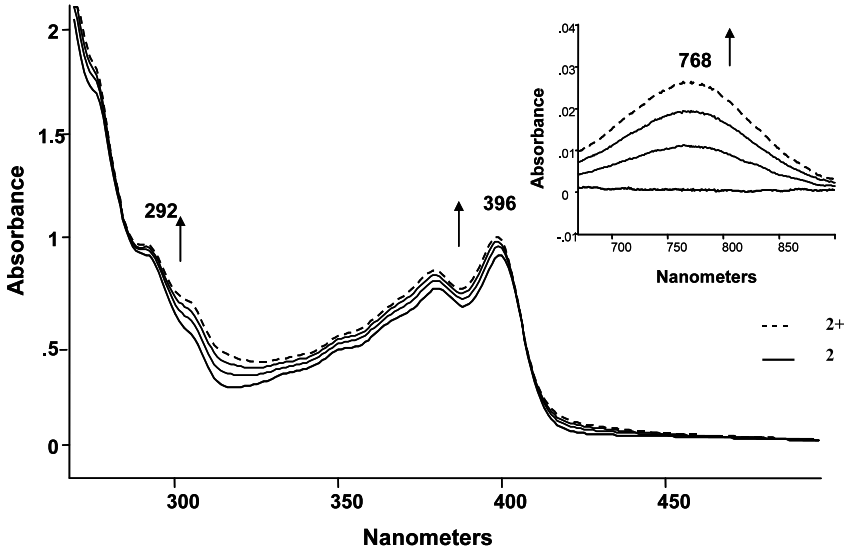

Fig. 1. UV–Vis spectral changes in an OTTLE cell during the oxidation of **2** in CH_2Cl_2 +0.1 mol l^{-1} TBAP, $c = 1.0 \times 10^{-3}$ mol l^{-1}, Pt, 20 °C.

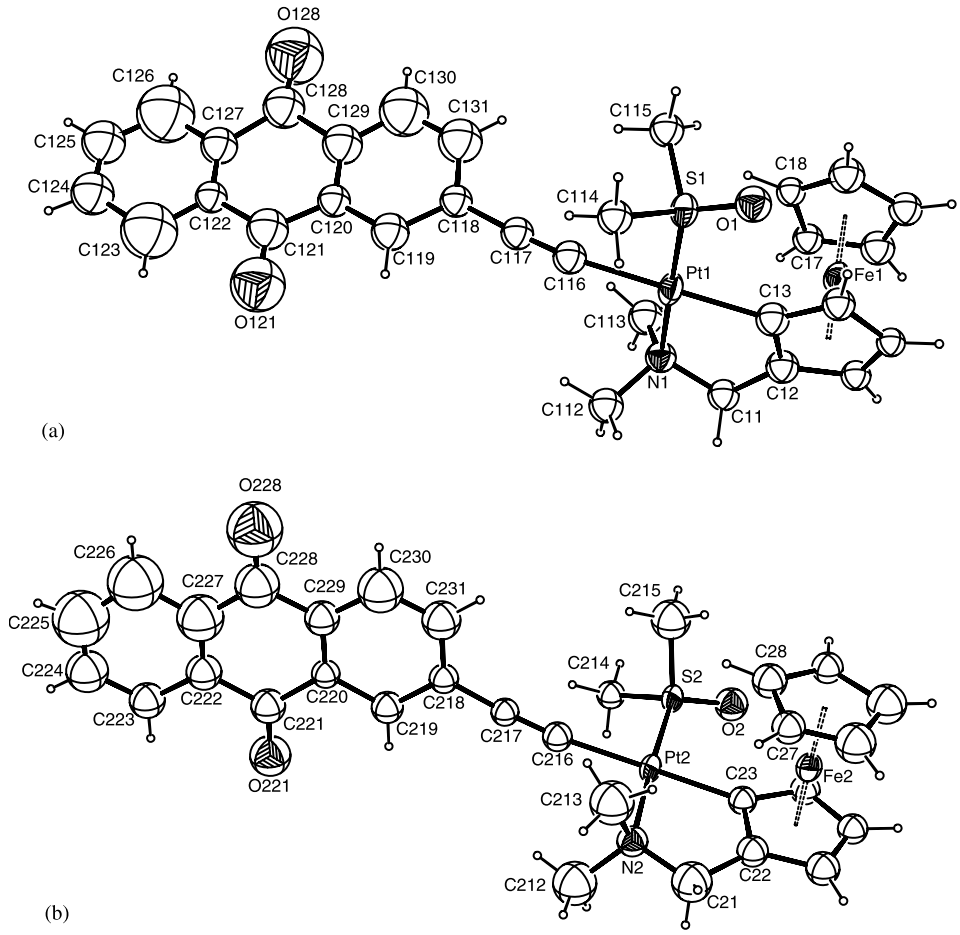

Fig. 2. Perspective views of the two unique molecules of **5** showing the atom numbering schemes with thermal ellipsoids drawn at the 50% probability level. For clarity only the first two atoms of consecutively numbered cyclopentadienyl rings are labelled. Molecule 1 of **5**. (b) Molecule 2 of **5**.

3.2. X-ray structure determination of **5**

The crystal comprises two unique molecules of **5** in the triclinic unit cell. A perspective view of both molecules of **5** is shown in Fig. 2 and defines the atom numbering schemes. Differences in bond lengths and angles between the discrete molecular units can be ascribed to crystal packing effects. The quality of the data obtained from the heavily twinned crystal (see experimental) precludes detailed comparison of the metrical data with the related molecules [Pt{(σ,η^5-$C_5H_3CH_2NMe_2$)Fe(η^5-C_5H_5)}(dmso)X, (X = –C≡C–$SiMe_3$, –C≡C-(η^5-C_5H_4)Fe(η^5-C_5H_5),[3] but the structure proposed for **5** is clearly confirmed from the crystallographic data. Selected bond length and angle data are given in Table 3 with data from molecule 1 used in the following discussion. The coordination sphere of the platinum atom comprises the S(1) atom of the S-bound DMSO ligand *trans* to the amine N(1) atom of the orthometallated ferrocenylamine ligand. The Pt-bound C(13) atom of the substituted cyclopentadiene ring is *trans* to the C(116) atom of the terminally bound 2-anthraquinoneacetylide, which occupies the fourth co-

Table 3
Selected bond lengths (Å) and bond angles (°) for **5**

Molecule 1		Molecule 2	
Bond lengths			
Pt(1)–C(13)	2.04(3)	Pt(2)–C(23)	2.00(2)
Pt(1)–C(116)	2.05(3)	Pt(2)–C(216)	2.02(3)
C(116)–C(117)	1.17(4)	C(216)–C(217)	1.19(3)
C(117)–C(118)	1.43(4)	C(217)–C(218)	1.45(3)
Pt(1)–S(1)	2.194(7)	Pt(2)–S(2)	2.182(6)
Pt(1)–N(1)	2.14(2)	Pt(2)–N(2)	2.12(2)
N(1)–C(11)	1.47(3)	N(2)–C(21)	1.45(4)
C(11)–C(12)	1.46(4)	C(21)–C(22)	1.47(4)
C(12)–C(13)	1.43(4)	C(22)–C(23)	1.46(3)
Bond angles			
C(13)–Pt(1)–N(1)	82.5(9)	C(23)–Pt(2)–N(2)	83.0(9)
C(116)–Pt(1)–N(1)	90.8(9)	C(216)–Pt(2)–N(2)	91.4(9)
C(13)–Pt(1)–S(1)	96.7(8)	C(23)–Pt(2)–S(2)	94.5(7)
C(116)–Pt(1)–S(1)	89.7(8)	C(216)–Pt(2)–S(2)	91.1(7)
C(13)–Pt(1)–C(116)	170.8(10)	C(23)–Pt(2)–C(216)	172.3(10)
N(1)–Pt(1)–S(1)	176.7(6)	N(2)–Pt(2)–S(2)	177.5(6)
C(117)–C(116)–Pt(1)	169(3)	C(217)–C(216)–Pt(2)	172(2)
C(116)–C(117)–C(118)	177(3)	C(216)–C(217)–C(218)	172(3)

ordination site. The N(1) and C(13) atoms are the donors in a five-membered chelate ring formed by the orthometallated ferrocenylamine ligand. Some deviation from the idealised square planar geometry about Pt is apparent with deviations from the PtL_4 ring plane ranging from −0.071(9) Å, Pt(1) to 0.04(1) Å, C(13).

The PtL_4 ring plane is inclined at an angle of 8.4(8)° to the plane of the cyclometallated cyclopentadienyl ring, while the anthraquinone ring plane is approximately orthogonal to both the coordination plane of the Pt atom, 76.8(8)°, and the cyclopentadienyl rings of the ferrocenyl moiety, 80(1)° to C(12)···C(16) and 81(1)° to C(17)···C(111). The cyclopentadiene rings in the ferrocenyl moiety adopt an approximately eclipsed conformation with the dihedral angle 3.7(8)° between the ring planes.

4. Conclusion

An analysis of the electrochemical and spectral data has enabled the HOMO and LUMO in these neutral cycloplatinated molecules with organic fluorophores to be defined; the HOMO is 'Fc' based whereas the LUMO is entirely fluorophore-centred. In principle, the cycloplatinated ferrocenylamine moiety offers an alternative to other organometallic species like ferrocene as a functional redox switch. In this case the on/off capability is related to the existence of charge-transfer states in the oxidised ferrocenium molecule and we have shown that low energy electronic CT transitions are a signature for this capability. But whether the acceptor orbital is largely ferrocenyl in character or has significant Pt(II) component is yet to be determined. Nevertheless, in comparison to analogous ferrocenyl compounds [6] there is only weak redox-switching capability.

Acknowledgements

We thank Dr. Amar Flood for some of the OTTLE measurements.

References

[1] (a) C.E.L. Headford, R. Mason, P.R. Ranatunge-Bandarage, B.H. Robinson, J. Simpson, J. Chem. Soc., Chem. Commun. (1990) 601;
(b) P.R.R. Ranatunge-Bandarage, B.H. Robinson, J. Simpson, Organometallics 13 (1994) 500.
[2] (a) P.R.R. Ranatunge-Bandarage, S.M. Johnston, N.W. Duffy, J. McAdam, B.H. Robinson, J. Simpson, Inorg. Chem. 13 (1994) 511;
(b) N.W. Duffy, M. Spescha, B.H. Robinson, J. Simpson, Organometallics 13 (1994) 4895.
[3] C.J. McAdam, E. Blackie, J.L. Morgan, S. Mole, B.H. Robinson, J. Simpson, J. Chem. Soc., Dalton. Trans. (2001) 2362.
[4] S. Fery-Forgues, B. Delavaux-Nicot, J. Photochem. Photobiol. A 132 (2000) 137.
[5] (a) Z. Wang, C. Kongchang, H. Tian, Chem. Letts. (1999) 423.;
(b) J. Gan, H. Tian, Z. Wang, K. Chen, J. Hill, P.A. Lane, M.D. Rahn, A.M. Fox, D.D.C. Bradley, J. Organomet. Chem. 645 (2002) 168.
[6] E.M. McGale, B.H. Robinson, J. Simpson, Organometallics 22 (2003) 931.
[7] A.R. Katritzky, W.H. Ramer, J. Org. Chem. 50 (1985) 855.
[8] M. Vlassa, I.A. Silberg, R. Custelceanu, M. Culea, Synth. Commun. 25 (1995) 3493.
[9] P. Nguyen, S. Todd, D. van den Biggelaar, N. Taylor, T. Marder, F. Wittmann, R. Friend, Synlett (1994) 299.
[10] C.J. McAdam, B.H. Robinson, J. Simpson, Organometallics 19 (2000) 3644.
[11] XSCANS, Area Detector Control and Integration Software, Bruker AXS, Madison WI, 1997.
[12] RLAT, Bruker AXS, Madison WI, 1997.
[13] G.M. Sheldrick, SHELXS-96, A Program for the Solution of Crystal Structures from Diffraction Data, University of Göttingen, Göttingen, Germany, 1996.
[14] G.M. Sheldrick, SHELXL-97, A Program for the Refinement Crystal Structures, University of Göttingen, Göttingen, Germany, 1997.
[15] K.A. Hunter and J. Simpson, TITAN2000, A Molecular Graphics Program to Aid Structure Solution and Refinement with the SHELX Suite of Programs, University of Otago, New Zealand, 1999.
[16] E.M. McGale, C.J. McAdam, unpublished work.
[17] (a) S. Niizuma, H. Kawata, Bull. Chem. Soc. Jpn. 66 (1993) 1627;
(b) P.H. Kasai, J. Am. Chem. Soc. 114 (1992) 2875.
[18] A. Klein, W. Kaim, Organometallics 14 (1995) 1176 (and references therein).